Dynamic-structure-factor measurements on a model Lorentz gas

P. A. Egelstaff
Physics Department, University of Guelph, Guelph, Ontario, Canada

O. J. Eder
Osterreichisches Forschungszentrum, Seibersdorf, Austria

W. Glaser
Technische Universität München, Garching bei München, Federal Republic of Germany

J. Polo
State University of New York, Alfred, New York

B. Renker
Kernforschungszentrum Karlsruhe, Institut für Nukleare Festkörperphysik, D-7500 Karlsruhe, West Germany

A. K. Soper
Rutherford Appleton Laboratory, Chilton, Didcot, United Kingdom
(Received 16 February 1989; revised manuscript received 11 September 1989)

A model system for the Lorentz gas can be made [Eder, Chen, and Egelstaff, Proc. Phys. Soc. London **89**, 833 (1966); McPherson and Egelstaff, Can. J. Phys. **58**, 289 (1980)] by mixing small quantities of hydrogen with an argon host. For neutron-scattering experiments the large H-to-Ar cross section ratio (~ 200) makes the argon relatively invisible. Dynamic-structure-factor [$S(Q,\omega)$ for H_2] measurements at room temperature have been made on this system using the IN4 spectrometer at the Institute Laue Langevin, Grenoble, France. Argon densities between 1.9 and 10.5 atoms/nm^3 were used for $0.4 < Q < 5$ Å^{-1}. Additional measurements were made with a He gas host at densities of 4 and 10.5 atoms/nm^3; helium is relatively invisible also compared to hydrogen. These experiments are described, and some examples of the results are presented to show the qualitative effects observed. The principle observation is a pronounced narrowing of $S(Q,\omega)$ as a function of ω as the argon density is increased. This effect is large at low Q and decreases with increasing Q, and also decreases substantially when helium is used in place of argon. In addition, the shape of $S(Q,\omega)$ is more complex than can be accommodated within a simple model, but slightly less complicated than a computer simulation so showing the significance of multiple-collision processes.

I. INTRODUCTION

The "Lorentz gas" is a distribution of infinitely heavy particles through which a light particle moves. It is believed that this is one of the more tractable and interesting problems in the kinetic theory of many-body systems. For many years it has been difficult to make detailed microscopic measurements on a system of this kind to compare to the theoretical predictions. If we adopt a large (~ 20) mass ratio rather than an infinite one, a mixture of a few hydrogen molecules in argon gas is an attractive experimental system. This is because the translational and rotational states of the hydrogen molecule are well separated and because the ratio of neutron-scattering cross sections (H_2-Ar) is abnormally large. Thus in a neutron-inelastic-scattering experiment the motion of single H_2 molecules can be followed fairly easily. Following the successful exploitation of the method by Eder, Chen and Egelstaff,[1] who used small quantities of hydrogen in liquid argon, a pilot experiment on the gas mixture at room temperature was conducted by McPherson and Egelstaff.[2] We have enlarged the gas experiments, covering a wider range of argon densities, and used fewer hydrogen molecules. In addition, we believe that we have made more accurate measurements of the dynamic structure factor. Our hydrogen density is similar to that used in the liquid argon work,[1] but the range of Q is much wider since the wavelength is less than half that of Ref. 1 and lower angles of scatter were available to us (4°–110° compared with 20°–90°). In addition, the argon density was varied, and the higher temperature of this experiment means that our data are much closer to the existing theoretical models which are based on hard-sphere or $r^{-\nu}$ interactions. Thus it is expected that the major qualitative features exhibited by a Lorentz gas may be demonstrated through these new data. The cross-section formulas for our case may be found in Appendix A.

The simplest phenomenon observed is the "cage effect," which was treated by a physical model in Ref. 1. If a hydrogen molecule is able to move freely, the dynamic structure factor $S(Q,\omega)$ will correspond to that for a perfect gas (where $\hbar Q$ and $\hbar\omega$ are the momentum and en-

ergy, respectively, transferred to the sample in a neutron-scattering experiment). But when enough argon is added to the system, the molecule will tend to be confined, or caged, by collisions with the argon. This effect will slow down its overall motion and lead to a narrowing in $S(Q,\omega)$ as a function of ω. In an extreme situation, we may reach a percolation limit. Thus the properties of multiple collisions are important in understanding these experiments. However, if the argon is exchanged for helium (10 times lighter), the cage effect is reduced as the masses of the molecule and the confining atoms are now similar. In this case, the width of $S(Q,\omega)$ shows much less reduction. In all cases the amount of this reduction in width compared to a perfect gas is a function of the momentum transfer ($\hbar Q$). If Q is small, large movements of the molecule are relevant and these may involve several collisions. For this case $S(Q,\omega)$ will be narrow and have a shape approaching the Lorentzian form. In contrast, for large values of Q, only small movements of the molecule are important and very few or no collisions will be significant, so that $S(Q,\omega)$ tends to a Gaussian shape and a width close to the perfect gas. Thus experiments need to be done over a range of parameters allowing a transition from Gaussian to Lorentzian limits.

For single-component gases the most important parameter affecting the neutron-scattering data is the mean free time or l/v, where l is the mean free path and v the mean velocity, and properties such as long-time tails in the time correlation functions are much less important. However, for the Lorentz gas it is expected that the long-time tail [classically $t^{-5/2}$ (Ref. 3) or quantum mechanically $t^{-3/2}$ (Ref. 4)] will be relatively more significant. Thus, if the observations correspond to the appropriate time scales, it may be anticipated that a more complicated shape would be seen at low ω in $S(Q,\omega)$ than predicted by a simple collision theory.[5,6] This feature will be demonstrated too.

There have been many theoretical papers about the properties of $S(Q,\omega)$ in a Lorentz gas. The most relevant here are those of Götze, Leutheusser, and Yip[6] and of Lackner and Posch[7] because they deal with the self-scattering law [$S_s(Q,\omega)$] for the light particle. Other theories that deal with the coherent scattering by the heavy particles (e.g., Letamendia, Nouchi, and Yip[8] are much less suitable. However, in all cases these theories do not handle realistic interatomic potentials, and are applicable either to hard spheres[6,8] or $r^{-\nu}$ potentials.[7] Also it is not clear which theory is to be preferred. We shall compare trends in the data to the work of Lackner and Posch[7] since the $r^{-\nu}$ potential is nearer to the high-temperature interactions for hydrogen and argon; but, in general, more theoretical work is needed for meaningful comparisons. In addition, we shall compare our results to computer simulation data[9,10] since these are the only results with moderately realistic potentials. They are, however, taken with infinite mass ratios, whereas in the theory of Lackner and Posch[7] the mass ratio can be set to the experimental value. Thus care is needed with all the theoretical comparisons.

In the next section we shall describe the experimental method, and in Sec. III the analysis of the data. Examples of $S(Q,\omega)$ to demonstrate the above effects will be given in Sec. IV.

II. EXPERIMENTAL METHOD AND DATA CORRECTIONS

The pressure vessels were those used in previous experiments on krypton[11,12] and the gas densities used are given in Table I. The spectrometer IN4 at the Institute Laue Langevin, Grenoble, was set to a wavelength of 1.6 Å (31 meV), but otherwise the experimental conditions for the krypton experiments[12] were unchanged. This change in wavelength was made because the energy transfers were expected to be significantly larger for hydrogen than krypton.

Measurements of the time-of-flight spectra at 100 angles between 4° and 110° were made for the empty pressure vessels and for vessels containing argon or helium only at each state shown in the table. Then the vessels were evacuated and filled with pure H_2 gas at 0.56×10^2 molecules/m^3 (about 20 atm), and after completing those measurements argon or helium was pumped into the hydrogen to generate the densities shown in the table. Measurements were also made, in one case, for a lower hydrogen density as a check and as a test for multiple scattering. Calibration measurements were made with a vanadium tube having the same dimensions and scattering power as a typical mixture.

Figure 1 is an example of the data at one angle, for argon plus the pressure vessel and for hydrogen plus the pressure vessel. This shows the large difference in the scattering due to the hydrogen even when the number of argon atoms greatly exceeds the number of hydrogen molecules. The data at each angle were converted to $S(Q,\omega)$ on an arbitrary scale using the methods described in Ref. 12. In place of the empty container term for the krypton work, we used the vessel plus argon data for our mixture cases. Then to obtain an absolute scale, the pure hydrogen results were compared to a calculation of $S(Q,\omega)$ for a perfect gas after an allowance was made for multiple scattering (see below). The calculation is described in Appendix A. The data at constant angle were converted to constant Q on an ω grid by an interpolation

TABLE I. Experimental densities ρ in 10^{27} molecules/m^3.

Density ρ		
Ar	He	H_2
3.90		0.56
		0.56
1.87		0.56
	4.06	0.56
		0.29
3.79		0.29
		0.56
	10.45	0.56
7.15		0.56
10.49		0.56

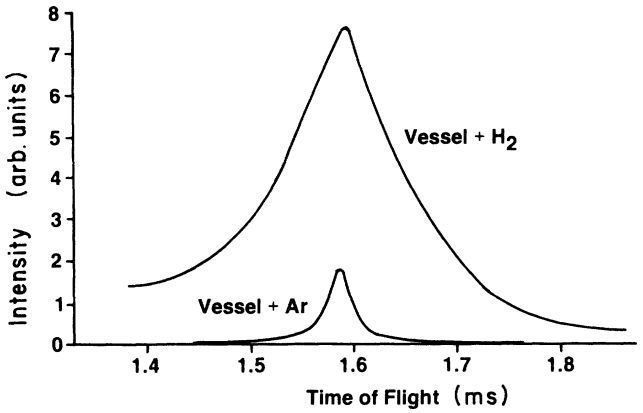

FIG. 1. Comparison of intensity (shown as a smooth curve through the experimental points) for the pressure vessel containing 3.9 atoms/nm^3 or argon (lower curve) with the vessel containing 0.56 molecules/nm^3 of hydrogen (upper curve) for a 1.6 Å neutron beam scattered at 21°.

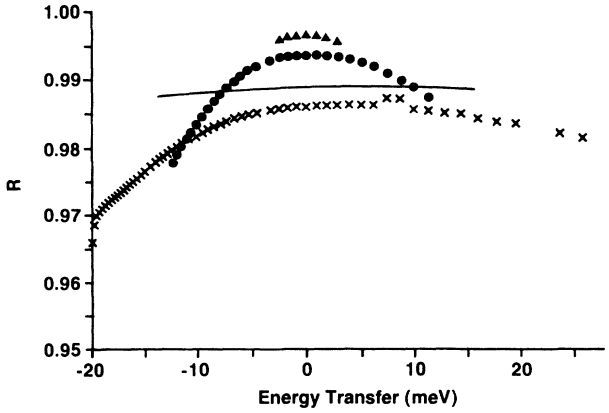

FIG. 3. Calculated results for the ratio of single scattering to the total of single plus multiple scattering: ▲ for 6°, ● for 12°, and × for 30°. The range of the points on the energy scale (see abscissa) corresponds to the extent of the observed single scattered intensity. The solid line is the experimental result for 9°, deduced from the data of Fig. 2.

procedure described in Appendix B.

In the case of this experiment the measurements of the pure hydrogen at two low pressures in the same vessel serve as a test of the degree of multiple scattering. Since the vessel is unchanged the scattering geometry will be unchanged. Because of the low density the scattering law is unchanged and, therefore, in doubling the hydrogen density, the multiple scattering will be doubled. Figure 2 shows the magnitude of this effect at an angle of 9°. It is seen that the differences are in the region of 1–2 %. To calculate this effect we used the methods described by Soper and Egelstaff,[13] except that the angular distribution of first scattering was taken into account. In order to perform this step at low angles a careful integration was necessary. The ratio of single scattering to the sum of single plus multiple scattering is shown in Fig. 3 for angles of 6°, 12°, and 30°. In each case the range of energy displayed corresponds to the range where the single intensity was found to be significantly different from zero. These data correspond generally with the experimental results at 9° shown by the solid line, but the calculated magnitude may be smaller. Nevertheless, the correction is clearly known to ~1% of the observed intensity.

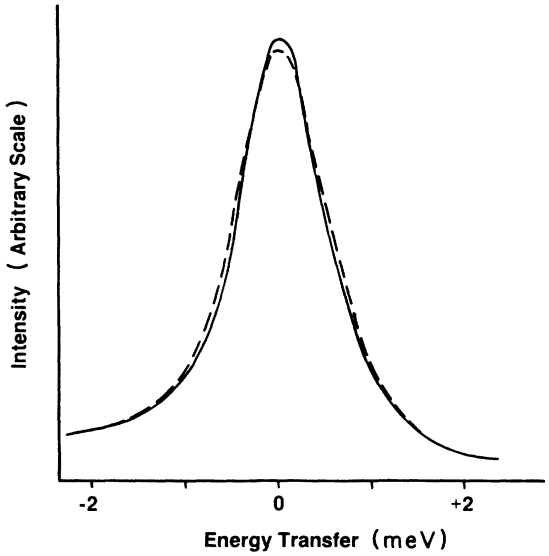

FIG. 2. Comparison of the normalized scattered spectra for hydrogen at 0.29 molecules/nm^3 (solid line) and 0.56 molecules/nm^3 (dashed line) using 1.6-Å neutrons at an angle of 9°. Because of the small differences the data are shown as smooth lines drawn through the experimental points.

The resolution function was determined from the vanadium data and had a width of 0.5 meV. It reduced the peak height at $Q=0.87$ Å, for example, by ~1%. Some examples of the experimental results will be shown later (Figs. 6 and 7), and it will be observed that the statistical fluctuations are relatively unimportant compared to systematic error due to uncertainties in the corrections discussed above. This error is difficult to estimate because if it was understood, a further correction would be made. However, from the uncertainties quoted above the systematic error is expected to be ~1%.

A table of the experimental results tabulated as a function of ω for given values of Q, may be obtained from the Physics Department, University of Guelph.

III. DISCUSSION AND COMPARISON WITH MODEL RESULTS

It is worth reviewing a single parameter presentation of the data to discover whether the experimental parameters allow the observations to extend from the region where free-particle behavior is important to the region where collision dominated behavior governs the shape of $S(Q,\omega)$. A suitable parameter is the product of peak height and half width at half maximum. This parameter varies from π^{-1} at low Q (Lorentzian shape) to $\sqrt{\ln 2/\pi}$ at high Q (Gaussian shape). Due to the influence of the

rotational and vibrational states of the hydrogen molecule, it is not expected to reach this upper limit at the limit of the experimental data ($Q \sim 5$ Å^{-1}). In practice, the data between 3 and 5 Å^{-1} were affected by Bragg reflections from the vessel and are not included in this survey. Figure 4 shows data of this kind for a number of cases. It is noticeable that the pure H_2 gas case does not vary with Q, staying close to the upper limit. We found that the H_2-He mixture also stays close to the upper limit, and we note that this parameter would be expected to fall for such cases at lower values of Q than those studied. In contrast, the two examples of H_2-Ar mixtures show a clear trend towards the lower limit as Q is reduced through the experimental range. At the higher argon density the Q range appears to cover the whole parameter range. Thus between $0.4 < Q < 3$ Å^{-1} this experiment surveys the appropriate set of behaviors for this model of a Lorentz gas.

Our data demonstrate very clearly the effect of changing the mass of the host atoms on the scattering from the light atom (hydrogen in our case). In Fig. 5(a) we compare the measured scattering curve of hydrogen in argon with that from hydrogen in helium at the same number densities for both hydrogen and heavier host atoms. The helium host clearly produces a greater width in $S(Q,\omega)$ and somewhat different shape near the peak. Of course, the atomic diameter of He is less than for Ar, so at least part of the measured spectrum changes might be attributed to size effects. However, the range of number densities

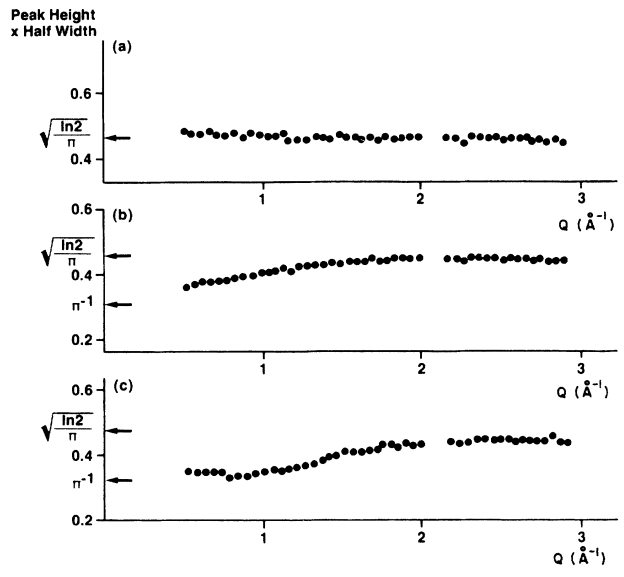

FIG. 4. Product of half width (HW) and peak height $S(Q,0)$ for several sets of data: (a) pure hydrogen at 0.5 molecules/nm^3, (b) a mixture of 0.5 H_2 molecules with seven Ar atoms per nm^3, (c) a mixture of 0.5 H_2 molecules with 10 Ar atoms per nm^3. Each curve should tend to the Lorentzian limits (π^{-1}) at low Q and to the Gaussian limit at very high $Q(\sqrt{\ln 2/\pi})$. For the H_2-Ar mixtures the data cover the bridging region fairly well, whereas for the H_2-He mixture and the pure H_2 the data lie near the higher Q limit.

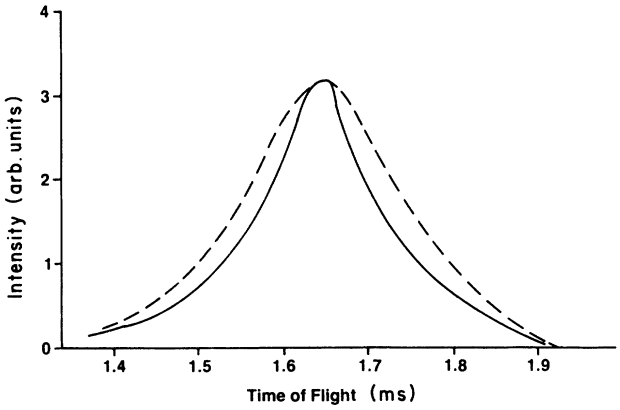

FIG. 5. Comparison of the shape of the constant angle data for the hydrogen scattering from mixtures 0.56 H_2+10.5 Ar and 0.56 H_2+10.5 He particles/nm^3. The full line has been drawn through the argon data and the dashed line through the helium data, for 1.6-Å neutrons at an angle of 21.8°. For this comparison the data were normalized to the same peak height.

at which data were taken for both argon and helium was such that we were also able to compare data from the two host atoms in the case where the Ar had the same free volume as the He, and a similar difference (not shown here) was seen. Therefore we concluded that in this case the mass, and not the size, of the host produces the predominant effect on the shape of the measured differential cross section.

It is interesting to compare the data to a sequence of models, the perfect gas (i.e., no collisions), a binary collision model (i.e., Ref. 5) and a model including all categories of collisions [i.e., a computer simulation (Refs. 9 and 10)]. In using these models and simulations we shall convert the calculated translational $S(Q,\omega)$ to the $S(Q,\omega)$ for hydrogen molecules by including rotational effects according to Eq. (A2). Also, the experimental resolution will be folded into these predictions before comparing to the experimental data. These comparisons are shown in Figs. 6–9. We begin with a comparison of a constant angle (21.8°) spectrum with the binary collision model; for this purpose we decided to employ the well-established models of Nelkin and Ghatak[5] (generalized to include quantum effects) and Egelstaff and Schofield.[14] These models involve only one parameter, the collision time. A reasonable fit was obtained at Ar densities of 1.87 and 3.90 atoms/nm^3, but not at the higher densities. An example using constant angle data at the highest density is shown in Fig. 6, and to emphasize the difference in shape we normalized each curve to have the same peak height. It can be seen that the model is more "rounded" in shape than the experimental data. This suggests that a second time, longer than the collision time, is needed in the interpretation. In Figs. 7, 8, and 9 we show several comparisons with the constant Q results. The perfect gas and binary collision models are compared to the experimental data for $Q = 0.87$ and 1.30 Å^{-1} in Fig. 7. Again it can be seen that we are unable to fit the data properly. As an illustration of the size of the effect being studied, it

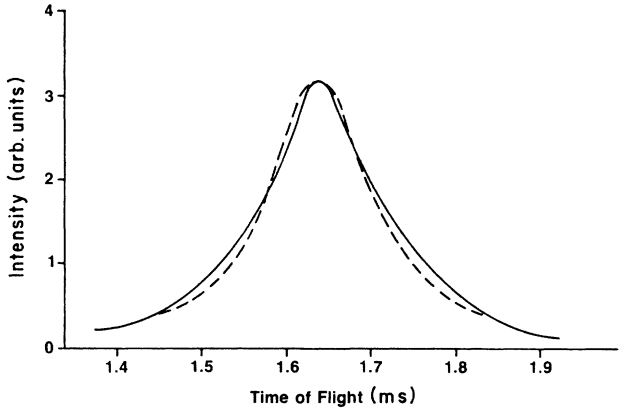

FIG. 6. Comparison of the shape of the constant angle data for the hydrogen scattering from a mixture of 0.56 H_2+10.5 Ar particles/nm^3 as in Fig. 5, solid line, and the best fit from the binary collision model, dashed line, normalized to the same peak height.

is useful to compare both experimental and model data to the perfect gas calculation (dashed line in this figure). It can be seen that, especially at the lower Q, the binary model allows for the larger part of the difference between the data and the perfect gas. However, by adjusting constants we were not able to obtain a good fit with the mod-

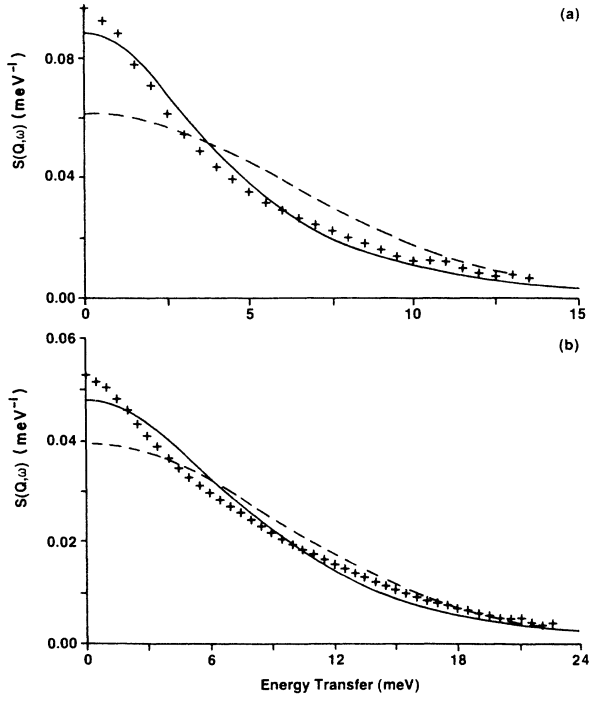

FIG. 7. Comparison of constant Q hydrogen data for the 0.56 H_2+10.5 Ar particles/nm^3 mixture. Plusses show the data, the dashed line shows the perfect gas result of Appendix A, and the solid line shows the binary collision model. In these examples the absolute normalization of $S(Q,\omega)$ and conversion to constant Q was used (see Appendix B). (a) $Q=0.87$ Å and (b) $Q=1.30$ Å.

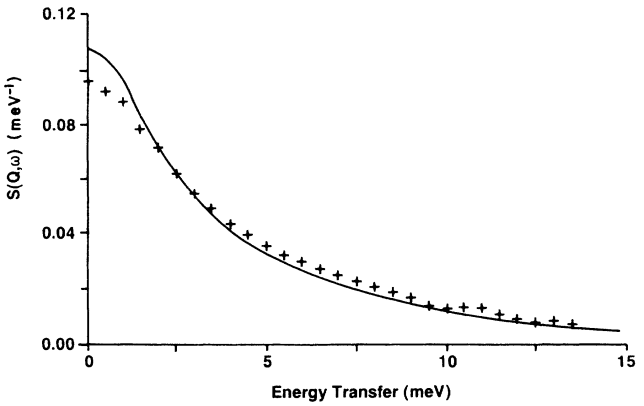

FIG. 8. Comparison of the experimental results of Fig. 7 (plusses) with the simulation data of Sharma *et al.* (Ref. 9) (solid line) for $Q=0.87$ Å^{-1}.

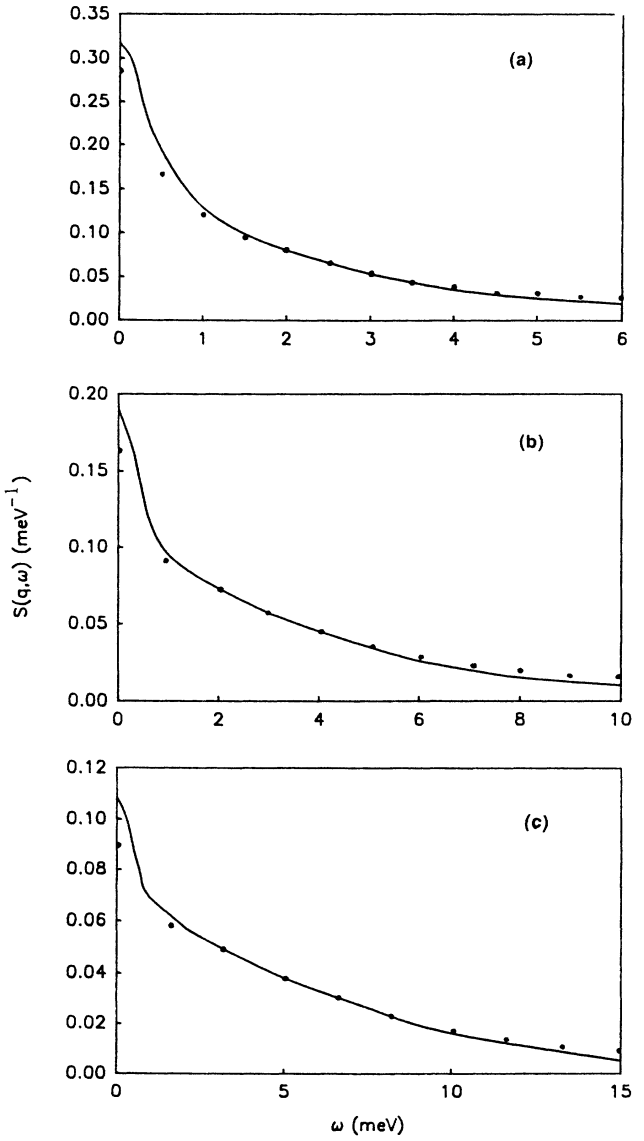

FIG. 9. Comparison of the experimental constant Q data (circles) at lower Q values with the simulation results of Joslin and Egelstaff (Ref. 10) (solid line). (a) $Q=0.5$ Å^{-1}, (b) $Q=0.7$ Å^{-1}, (c) $Q=1.0$ Å^{-1}.

TABLE II. Summary of peak heights and widths for the models of Lackner and Posch (Ref. 7).

Potential	HS	r^{-12}	r^{-4}	r^{-4}	Expt.
Mass ratio	∞	∞	∞	20	20
Peak heights (units[a] of $Q^*/\omega\tau$)					
$Q^*=0.5$	1.6	2.0	3.9	1.8	1.5
$Q^*=1.0$	1.1	1.2	2.0	1.2	1.1
Full widths at half-maximum (units[a] of $\omega\tau/Q^*$)					
$Q^*=0.5$	0.45	0.3	0.07	0.35	0.32
$Q^*=1.0$	0.75	0.6	0.17	0.55	0.6

[a] $\tau=MD/k_BT$, $Q^*=2DQ^2\tau$, and D is the impurity self-diffusion coefficient.

el and have concluded again that an additional longer time is required also.

Two studies have been carried out, using the molecular dynamics simulation technique, by Sharma *et al.*[9] and by Joslin and Egelstaff.[10] In both cases the idealized host (of infinite mass atoms) was used and the hydrogen-argon Lennard-Jones potential was used between a light test particle and the host. It is known from the work of LeRoy and Hutson[15] on realistic potentials that the isotropic Lennard-Jones function is approximately correct. The computer simulation studies have shown that the qualitative effects discussed above are similar to those observed; thus they confirm the appropriateness of H_2-Ar mixtures for an experimental test of the Lorentz gas. As an example, we compare in Fig. 8 the data of Fig. 7(a) with the simulation of Sharma *et al.*[9] It can be seen that the simulation is more peaked at low ω than the data in contrast to the models in Fig. 7(a), which show the opposite behavior. Thus the role of higher-order collisions is important. However, the simulation Q's are not low enough in this case to examine a very large system. Somewhat lower values of Q and a higher quality simulation were used by Joslin and Egelstaff.[10] Figure 9 shows their lowest three Q values. In Fig. 9(a) for $Q=0.5$ Å^{-1} the calculated curve is a good fit to the data for $\omega>1$ meV, but becomes more peaked at lower ω. At higher Q values—Figs. 9(b) and 9(c)—the data extend to higher values of ω and this effect decreases somewhat. Again this simulation comparison confirms that multiple collisions play a significant role.

It is known (Ref. 7, for example) that decreasing the mass ratio from infinity to the experimental value of 20 will reduce the cage effect, and also that its magnitude depends on the softness of the interatomic potential. The available theoretical results are compared to experiment in Table II; for our highest density the values of Q^* are similar to the values of Q in Å^{-1}. Thus the differences between the simulations of Figs. 8 and 9 and the experimental results might be explained by the reduced mass ratio since the H_2-Ar interaction[15] is about as rigid as the Lennard-Jones potential.

IV. CONCLUSIONS

We have in this series of experiments, demonstrated in some detail that a mixture of H_2 in Ar forms a good experimental model of the Lorentz gas, and that the technique of neutron scattering enables the detailed dynamics to be studied and the principal phenomena predicted by theory to be observed. In this paper we have extended and enlarged on our earlier experiments.[1,2] More detailed analysis of these data, including more comparisons with computer simulations, would be justified. It is unfortunate that the theoretical work[6,7] does not allow detailed predictions to be made, and that quantitative analysis is difficult because the competing effects due to changes in mass ratio and uncertainties in the interaction potential may not be fully disentangled at present. Both improvements to the experiment and the theoretical predictions would be worthwhile. In particular, work at lower Q would be expected to test the percolation limit aspect of this work, and severely test improvements in the theoretical predictions.

ACKNOWLEDGMENTS

The support of the Natural Sciences and Engineering Research Council of Canada is gratefully acknowledged. We would also like to thank the Institute Laue Langevin Grenoble, France for their support of this program.

APPENDIX A: CALCULATION OF $S(Q,\omega)$ FOR HYDROGEN GAS

The cross section of hydrogen gas at room temperature is mainly incoherent ($\sim$96%), and so is usually[16,17] written as

$$\frac{d^2\sigma}{d\Omega d\delta}=\sum_{J,J'}\left[\frac{d^2\sigma}{d\Omega d\omega}\right]_{JJ'}$$
$$=\sum_{J,J'}\frac{k}{k_0}a^2(\mathbf{Q},J,J')S_T(\mathbf{Q},\omega-\omega_{JJ'})\ . \qquad \text{(A1)}$$

Here the subscript J,J' represents the partial cross section for the rotational transition $J\rightarrow J'$. $\mathbf{Q}=\mathbf{k}_0-k$, is the momentum transfer in units of $\hbar$, $\mathbf{k}_0$, and $\mathbf{k}$ are the initial and final wave vectors, respectively. $\hbar=\hbar^2(k_0^2-k^2)/2m$ is the energy transferred to the system in the scattering process. $\hbar\omega_{JJ'}=B(J'(J'+1)-J(J+1))$ represents the rotational energy gain with the quantum numbers J and J'. The Pauli principle requires that J be even when the total nuclear spin $I=(I_1+I_2)$ of the Hydrogen molecule is zero (parahydrogen), and that J be odd when I is 1 (orthohydrogen). B is the rotational constant, while $a^2(Q,J,J')$ plays the role of an effective incoherent scattering length. This equation may be reduced to a convolution

$$S(Q,\omega)=\int S_R(Q,\omega')S_T(Q,\omega-\omega')d\omega'\ , \qquad \text{(A2)}$$

where ω' corresponds to the rotational energy states of the hydrogen molecule and $S_T(Q,\omega)$ and $S_R(Q,\omega)$ are the translational and rotational contributions. $S_R(Q,\omega)$ will be calculated by the free-molecule expression given, for example, by Young and Koppel[16] or Sears.[17] For the

free-gas case $S_T(Q,\omega)$ is given by the usual expression for a perfect atomic gas. However, we also considered the binary collision model of Nelkin and Ghatak,[5] which we generalized to include quantum effects to first and second order. A program was written for this expression and we found that it gave results identical to the simpler, but *ad hoc,* model of Egelstaff and Scofield.[14] In the comparisons with experiment, we shall use the latter model. The computer simulations[9,10] also yield $S_T(Q,\omega)$, which is used then in Eq. (A2) to calculate $S(Q,\omega)$ to compare to our experimental results.

APPENDIX B: EXPERIMENTAL DATA AT CONSTANT Q FROM THAT AT CONSTANT ANGLES

In a neutron-scattering experiment, the basic energy and momentum conservation relation is

$$\frac{\hbar^2 Q^2}{2m} = 2E_0 + \hbar\omega - 2\sqrt{E_0(E_0+\hbar\omega)}\cos\alpha \ , \qquad \text{(B1)}$$

where α, $\hbar\omega$, E_0 and m are, respectively, the angle of scattering, the energy transfer, the incident energy, and the mass of the neutron. In order to convert the experimental data at constant angles to that at constant wave vector Q_c, we adopted the following procedure. For each wave vector Q_c and each energy value $\hbar\omega$ (positive or negative), an angle α_+ (or α_-) was found from the above equation. For this α_+ (or α_-) a new set of data for $S(Q,\omega)$ (that is, ω and Q for each experimental time channel) was obtained by linearly interpolating between two sets of time-of-flight experimental values associated with two experimental angles, the one just above and the other one just below α_+ (or α_-). This would correspond to the experimental result for the angle α_+ (or α_-). Then Eq. (A1) was used to calculate two (sometimes only the one previously chosen) values of energy, say ω_1 and ω_2, at the constant wave vector Q_c and the angle α_+ (or α_-). The experimental table for the angle α_+ was utilized to get $S(Q,\omega_1)$ at ω_1 from a smooth parabolic ($=A\omega^2+B\omega+c$) five-point fit, with A, B, and C as three parameters at ω's near ω_1. Similarly, $S(Q,\omega_2)$ at ω_2 was also obtained from the same table. The whole procedure was repeated for equal intervals of energies, starting from zero, and a complete set of $S(Q,\omega_1)$ versus ω_1 at constant Q_c was obtained. It turned out that the set of $S(Q,\omega_1)$ versus ω_1 for all the positive values of $\hbar\omega$ selected at equal intervals yielded sufficient data.

[1] O. J. Eder, S. H. Chen, and P. A. Egelstaff, Proc. Phys. Soc. **89**, 833 (1966).
[2] R. McPherson and P. A. Egelstaff, Can. J. Phys. **58**, 289 (1980).
[3] M. H. Ernst and A. Weyland, Phys. Lett. **34A**, 39 (1971).
[4] W. Hoogeveen and J. A. Tjon, Physica A **125**, 163 (1984).
[5] M. Nelkin and A. Ghatak, Phys. Rev. **135**, A4 (1964).
[6] W. Götze, E. Leutheusser, and S. Yip, Phys. Rev. **23**, 2634 (1981).
[7] T. Lackner and M. Posch, Phys. Rev. A **36**, 5401 (1987).
[8] L. Letamandia, G. Nouchi, and S. Yip, Phys. Rev. A **32**, 1082 (1985).
[9] K. C. Sharma, S. Ranganathan, P. A. Egelstaff, and A. K. Soper, Phys. Rev. A **36**, 809 (1987).
[10] C. Joslin and P. A. Egelstaff, J. Stat. Phys. **56**, 127 (1989).
[11] A. Teitsma and P. A. Egelstaff, Phys. Rev. A **21**, 367 (1980).
[12] P. A. Egelstaff, W. Gläser, D. Litchinsky, E. Schneider, and J-B. Suck, Phys. Rev. A **27**, 1106 (1983).
[13] A. K. Soper and P. A. Egelstaff, Nucl. Instrum. Methods **178**, 415 (1980).
[14] P. A. Egelstaff and P. Schofield, Nucl. Sci. Eng. **12**, 260 (1962).
[15] R. J. LeRoy and J. M. Hutson, J. Chem. Phys. **86**, 837 (1987).
[16] J. A. Young and J. U. Koppel, Phys. Rev. **135**, A603 (1964).
[17] V. Sears, Proc. Phys. Soc. **86**, 953 (1965); **86**, 965 (1965).